



Geological Survey Paper 21:

Detrital provenance of quartzite facies in the Northern Tyennan Domain

Authors: G. Cumming, C. Jackman, R. Berry, I. Port,
S. Armistead and C. Carrasco Godoy
Date: 11/03/2026
Email: info@mrt.tas.gov.au
Website: www.mrt.tas.gov.au



Borradaile Creek, Northern Tyennan Region.

REPORT NO.: GSP21



Abstract

Detrital zircon U-Pb geochronology from quartzite and quartz-mica schist of the Mersey Metamorphic Complex provide new constraints on sediment provenance in the Northern Tyennan region. Both samples record broad Palaeoproterozoic age populations (1.6–1.9 Ga) and a consistent Mesoproterozoic component at ~1.45 Ga, indicating a detrital zircon provenance from long lived Palaeoproterozoic crust with subordinate Mesoproterozoic input. The age spectra of both samples correspond closely to those observed from successions in the western Rocky Cape Group and Palaeoproterozoic zircon-rich units within the Tyennan Block elsewhere. The Arm River sample (R030085) is dominated by a ~1.72 Ga population with a subordinate ~1.45 Ga mode, closely matching the Detention Subgroup and Lagoon River Quartzite. The Dublin Plain sample (R030082) exhibits comparable age components but aligns most strongly with the Pedder River Siltstone and Balfour Subgroup. Similar age provenance signatures are observed in the Red Point Complex, Needles Quartzite, Tyennan Quartzite, and the Strathgordon Metamorphic Complex. These results establish robust Palaeoproterozoic–Mesoproterozoic provenance links between the Northern Tyennan region and western Proterozoic successions of Tasmania and refine constraints on sediment sourcing prior to Cambrian deformation.

Detrital provenance of quartzite facies in the Northern Tyennan Domain

G. Cumming¹, C. Jackman¹, R. Berry², I. Port³, S. Armistead² and C. Carrasco Godoy²

¹ Geological Survey Branch - Mineral Resources Tasmania, Australia

² Centre for Ore Deposit and Earth Sciences (CODES), University of Tasmania, Australia

³ Weizmann Institute of Science, Rehovot, Israel

ARTICLE INFO

Published: 11/03/2026
Publisher: MRT
Report No.: GSP21

KEYWORDS

Mesoproterozoic
Zircon
U/Pb ICPMS
Mersey River Metamorphic
Complex

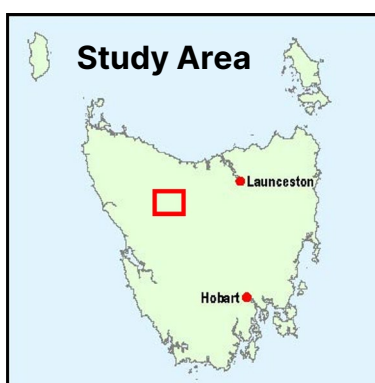
INTRODUCTION

Regional Geology

The Proterozoic geological history of Tasmania is marked by a complex interplay of sedimentation, rifting, and tectonic deformation. Mesoproterozoic marine siliciclastic sequences and Neoproterozoic rift-related deposits are preserved across regions such as King Island, Rocky Cape, and Western and north-western Tasmania. These rocks were later structurally modified during the Cambrian Tyennan Orogeny, resulting in overthrust relationships that now define the Tyennan Domain. The Tyennan Domain extends from the Borradaile, Cradle Mountain and Lake Rowallan region in the north, to far south-western Tasmania ([Figure 1](#)).

Despite broad correlations with formations like the Rocky Cape Group and Neoproterozoic units, the internal structure and stratigraphy of the Tyennan Domain remain poorly resolved. Detrital zircon geochronology has emerged as a tool for resolving the depositional history and provenance of deformed and metamorphosed units. Previous studies have laid the groundwork for zircon-based stratigraphic frameworks (Halpin et al., 2014 and Mulder et al., 2019), but sample analysis within the Tyennan Domain, particularly the northern part, has been sparse.

This study presents the provenance and age constraints of two new detrital zircon samples from quartzose rocks near Dublin Plain and Mersey Forest and aims to establish some baseline data in order to determine the initial provenance signatures of the Northern Tyennan. This study aims to a) constrain the maximum stratigraphic ages of quartzite-bearing facies in the Mersey Forest-Lake Dublin Road areas, and b) compare the new results of previous detrital zircon studies for the Tyennan Domain (Halpin et al., 2014; Black et al., 2004 and Mulder, 2013) with less deformed Proterozoic rocks in Tasmania (Mulder et al., 2018; Halpin et al., 2014 and Black et al., 2004).



Geological setting of the northern Tyennan Region

Medium-grade metamorphic rocks occur along the northern margin of the Tyennan Block, especially in the upper Mersey River region and parts of Cradle Mountain. The Mersey and Forth River areas were first mapped by Spry (1958) for the Hydro-Electric Commission between 1955 and 1956. Spry documented a ~4.2 km-thick succession of quartzite, mica schist, phyllite and slate, and noted the absence of repeated stratigraphic units around fold limbs, which he attributed to a mechanism he termed “strike-faulting.” Although he attempted to subdivide the region into lithological groupings (the Dove, Fisher and Howell Groups), he recognised the inherent difficulty in defining consistent stratigraphic divisions.

Jennings (1963) subsequently reassessed these groupings while mapping the Middlesex sheet, concluding that several of Spry’s units were not lithologically distinguishable. In particular, the Maggs Quartzite and Arm Schist could not be reliably differentiated from the Dove Schist or Fisher Group, leading Jennings to question the validity of the original subdivisions. He also found no demonstrable continuation of the Howell Group beyond the Mersey and Arm Rivers.

Turner (1989) later reinterpreted the units as metamorphic complexes rather than stratigraphic groups. Berry et al. (2007) then unified Spry’s three units into the Mersey River Metamorphic Complex, arguing that the internal divisions were not mappable at a meaningful scale. They retained the name Dove Schist for the dominant schistose unit following Spry’s original terminology. Although the metamorphism in the Mersey region had not been directly dated then, Meffre et al. (2000) suggested that the metamorphism within the complex was likely Cambrian in age, based on similarities in lithology, metamorphic assemblage and structural configuration to the Port Davey Metamorphic Complex.

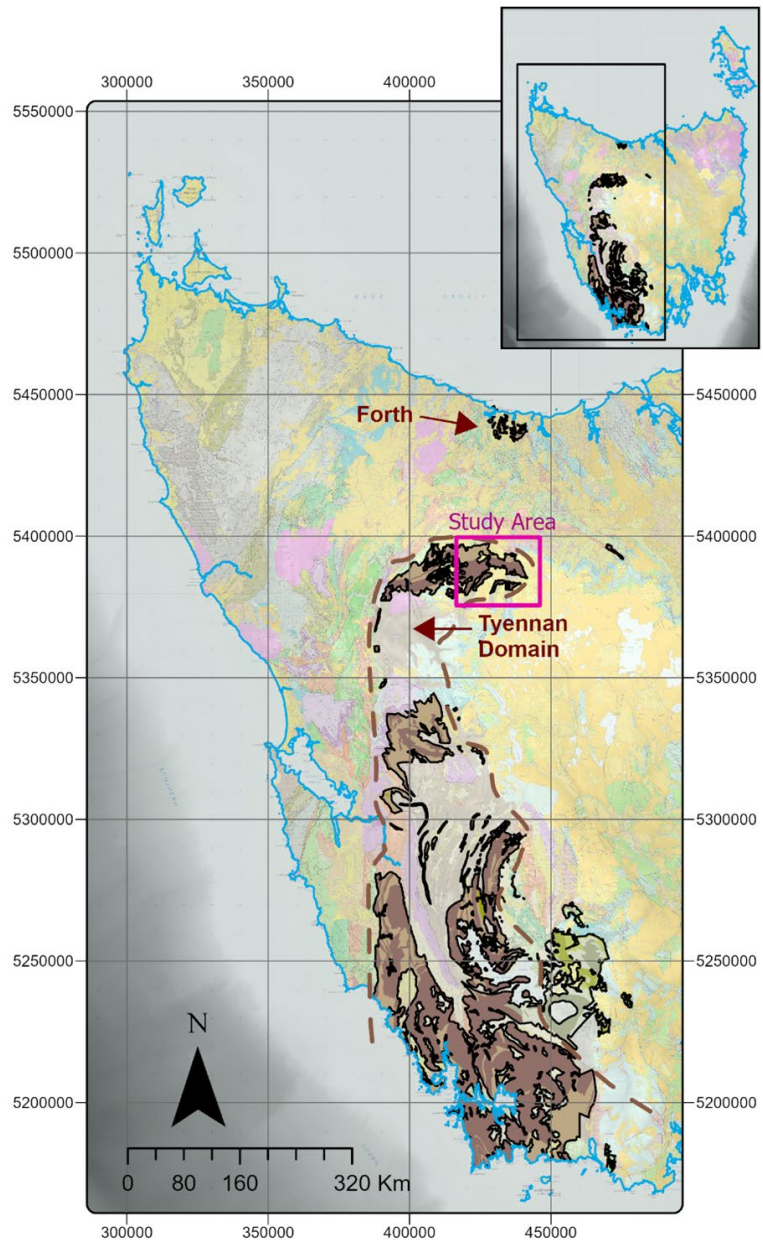


Figure 1. Western Tasmania, showing the extent of Tyennan Region, the Forth Metamorphic Complex and the study area as shown. Detailed lithologic information for the study area is shown in [Figure 2](#).

More recently, Mattner’s 2015 mapping of the Lake Rowallan shoreline confirmed that the structural history of the area aligns with that of other Cambrian medium grade metamorphic complexes in western Tasmania. She identified inclusion trails in garnet and albite porphyroblasts that preserve early deformation fabrics, as well as recumbent folding, compositional banding and later upright folding. Mineral chemistry indicates peak metamorphic conditions of ~550 °C and ~7.2 kbar, consistent with subduction-related metamorphism prior to exhumation. Mattner attributed the development of open upright folds to a later D₃ deformation event and interpreted subsequent shearing as part of a D₄ phase.

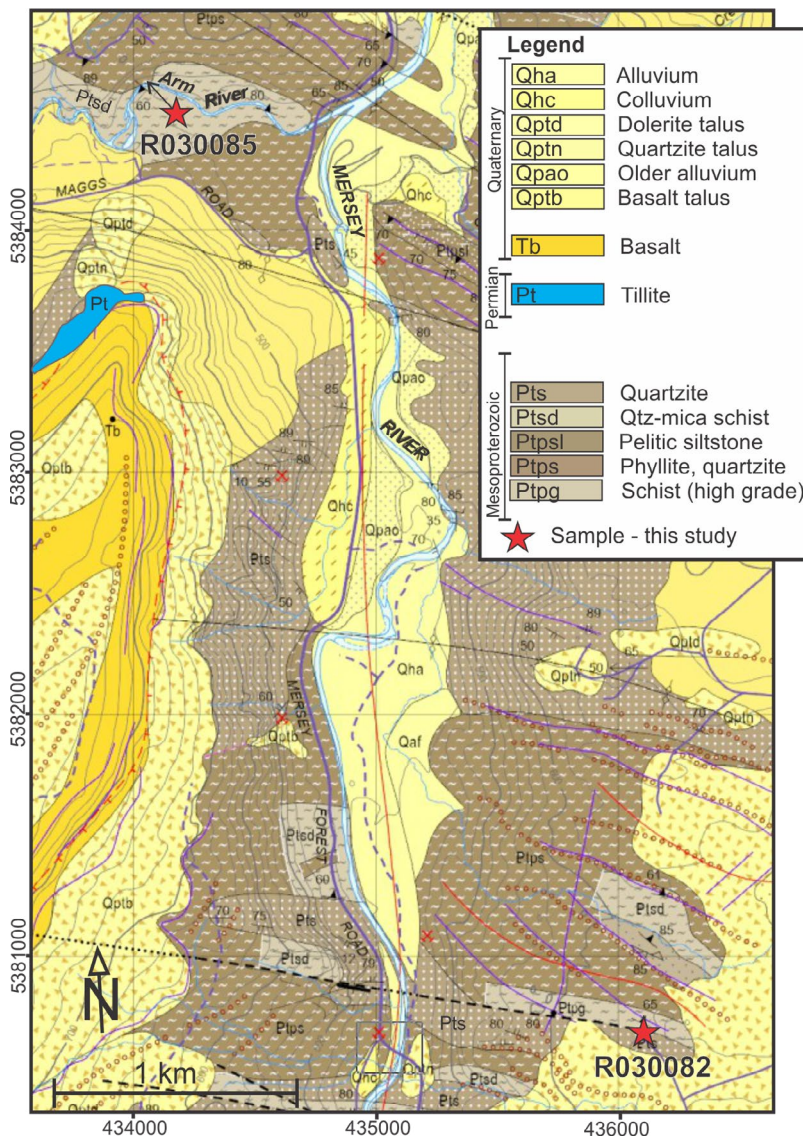


Figure 2. Geological map based on the preliminary compilation of geological mapping traverses (Cumming, in prep., 2026) of the area between Mersey Forest and Dublin Plain with sample locations.

The P–T trends of the Mersey River Metamorphic Complex align with this interpretation of moderate-grade Cambrian metamorphism. Monazite dating from the Mersey River Metamorphic Complex ($\sim 497 \pm 3$ Ma) places metamorphism at the younger end of the Tyennan Orogeny (Chmielowski and Berry, 2012). Unlike adjacent high-pressure complexes such as the Franklin and Port Davey blocks, which record steep burial to eclogite-facies conditions followed by rapid isothermal decompression, P–T indicators from the Mersey region show medium-grade, greenschist to transitional amphibolite-facies assemblages, with no evidence of high-pressure (>1.0 GPa) metamorphism. This suggests metamorphism occurred at shallower levels within the orogenic system, consistent with its structural position on the northern Tyennan margin. The P–T trajectory is there-

fore interpreted as a moderate-P, moderate-T path, lacking the extreme loading and unloading cycles observed in the high-pressure core of the orogen (Chmielowski and Berry, 2012).

Mattner (2015) also noted that the patchy distribution of garnet throughout the Lake Rowallan region may reflect chemical variability within the protolith, or localised metasomatic enrichment resulting in selective development of garnet despite uniform regional P–T conditions.

Lithostratigraphic units of the study area

The Northern Tyennan region was geologically mapped during the 2021–2025 field seasons as part of a Geological Survey of Tasmania campaign covering the Borradaile, Liena and Lake MacKenzie 1:25 000 map sheets (Cumming, in prep., 2026). This work sought to refine the stratigraphic and structural framework of the area and to clarify the internal variability of the metamorphic successions.

Mapping identified three broad lithostratigraphic units within the Borradaile–Liena area. These units are typically gradational or bounded by faults and, due to intense folding, pervasive strain and segmentation by narrow shear zones, they are not continuously mappable. Most lithologies occur as discontinuous slivers and lenses and, as recognised by earlier workers, cannot be divided into discrete stratigraphic members. Despite this complexity, three recurring facies associations can be distinguished based on preserved sedimentary features, lithological components and metamorphic grade.

The quartzite facies association (mapped as Pts in Cumming, in prep., 2026; Figure 2) comprises dominantly quartzite with subordinate phyllite and pelite. It typically exhibits lower to upper greenschist-facies mineralogy and variable strain. Subunits include massive quartzite (Lts) and foliated quartz-mica schist or micaeous metaquartzite (Ltsd).

The pelitic and phyllitic facies association (units Ltps, Ltp, Ltps-rcg) is also lower-to-upper greenschist-facies and displays variable strain intensity. This association includes interlayered or banded phyllite and quartzite (Ltps), phyllite-dominated intervals (Ltp), and low strain pelitic successions (Ltps-rcg), the latter preserving lenticular-bedded to banded siltstone, minor quartz sandstone, gutter casts, sand-filled cracks and occasional pebbly layers.

The schistose facies association (unit Ltpg) represents the highest metamorphic grade in the area, extending from upper greenschist into middle amphibolite-facies. These rocks are fine- to coarse-grained pelitic schists, commonly thinly banded and garnetiferous, with typical mineral assemblages including phengite, biotite, almandine, albite and chlorite. They commonly coincide with zones of elevated strain, pervasive recrystallisation and well-developed schistosity.

Study Area and Sample Selection

The Mersey and Arm River areas near Mersey Forest, south of Lake Parangana, contain exposures of planar-bedded, upright folded and variably sheared quartz-mica schist and quartzite. The least weathered and least sheared quartzite and quartz-mica schistose dominated outcrops were targeted for geochronology because of their presumed abundance of dateable minerals. Samples were collected from two localities: Arm River and Dublin Plain (Figure 2). The Arm River sample was collected from quartzite exposures situated on outcrops in Arm River, upstream of the confluence between the river and Lake Parangana. The Dublin Plain sample was collected from low outcrops at the termination of an old forestry road. Samples were selected for zircon U-Pb dating following petrographic and geochemical examination. Sample details and geological context are summarised in [Table 1](#).

Sample R030082

Sample R030082 is a quartz-muscovite schist ([Figure 3a](#)) collected from an outcrop of strongly foliated, finely laminated quartz-mica schist with well developed, fine-grained compositional layering shown as alternating lighter and darker bands (mapped as Ptpg in Figure 2; Cumming, in prep., 2026). Foliation surfaces are tight and gently undulating (Figure 3a). The foliation is continuous and anastomosing, but locally segmented, implying ductile

strain accompanied by moderate metamorphic recrystallisation. Isolated fold hinges in quartz veins occur along the dominant foliation (indicated as arrows in Figure 3a). These features indicate high ductile strain with transposition of pre- to early syn-deformational quartz veins. An east-west trending fault or shear is recorded just south (100-200 m) of the sample. The exposure has also been scoured and modified by Pleistocene glacial carving.

In thin section, R030082 contains quartz, albite, muscovite, chloritoid and biotite, consistent with upper greenschist facies metamorphism ([Figure 4b](#)). The rock comprises a fine- to medium-grained quartz matrix dominated by elongate, sutured quartz grains aligned parallel to foliation. Muscovite forms thin, brownish to pale yellow laths that define the foliation and occur in discrete micaceous domains. Chloritoid grains (pale green grey with characteristic pleochroism) are sparsely distributed throughout the rock. Strain shadows and pressure solution seams occur along the foliation, reflecting low grade metamorphic deformation. The resulting lepidoblastic to granoblastic texture is typical of quartz-mica greenschist facies rocks (Figure 4a).

Under cross polarised light (Figure 4a), quartz shows mosaic extinction patterns and pervasive undulose to sweeping extinction, indicating sub-grain development and dynamic recrystallisation. Muscovite occurs as brightly coarse-grained prismatic flakes. Chloritoid is mostly equant, consistent with growth during greenschist facies metamorphism. Small muscovite-chloritoid-quartz aggregates locally form brightly coloured streaks. A notable feature of this sample is the presence of large, rotated albite porphyroblasts (Figure 4a, b and c), with curved inclusion trains (S1).

Sample R030085

Sample R030085 is a quartzite comprising quartz, muscovite and chloritoid, recording low-grade greenschist facies metamorphic assemblages. It is fine-grained (<0.5 mm) and exhibits a pervasive metamorphic overprint. The sample was collected from outcrops of quartzite near the contact between quartz-mica schist (Ptsd) and alternating quartzite and interlayered quartzite and phyllite (Ltps and Ptsd; in Cumming, in prep., 2026), several hundred metres upstream from exposures of quartzite breccia. Outcrops lie within the hinge line and central part of an east-west trending shear lozenge and display well developed kink folding and associated deformation fabrics.

These exposures contain pronounced kink bands and transposition layering, likely reflecting differentiated strain and minor compositional banding in the quartzite dominated facies.

The quartzite is well sorted and finely (<0.5 mm) recrystallised, with a strain affected fabric typical of low grade shear zone deformation. Photomicrographs (Figure 4e and f) show a mosaic of fine, equant quartz grains, many exhibiting undulose extinction and sub-grain development, evidence of dynamic recrystal-

lisation. Grains display subtle grain boundary migration and patchy extinction domains consistent with low temperature mylonitic reworking. Sparse muscovite forms fine, aligned laths, while chloritoid is present as low order grey blue interference colour grains (at higher magnification), and are irregular to slightly elongate, occurring as isolated crystals or small clusters.

A discrete foliation plane or shear band is visible as a narrow, darker micaceous seam cutting across otherwise granoblastic quartz domains (Figure 4f).

Table 1. Locations and rock types dated from the Northern Tyennan. Coordinates are quoted in GDA94Z55.

Sample Number	Locality	Rock Type	Litho-stratigraphic Unit
2024-G-610 R030082	436093 mE/5380707 mN Borradaile. Field station 1701, Dublin Plain	Quartz-muscovite schist	Mersey Metamorphic Complex
2024-G-611 R030085	434050 mE/5384589 mN Borradaile. Field station 1791. Arm River	Quartzite	Mersey Metamorphic Complex



Figure 3. Photographs showing outcrops of quartz sandstone sampled from the Northern Tyennan for geochronology. a) Quartz-mica-albite schist from near Dublin Road (Sample R030082). The outcrop is strongly foliated with finely laminated compositional layering with alternating light and dark bands. Foliation is continuous, anastomosing and locally segmented, with small fold hinges and entrained, segmented quartz veins or bands visible along the main foliation surface (indicated with red arrows). Outcrop has been smoothed and modified by Pleistocene glacial abrasion. b) Folded, thinly bedded quartzite (R030085) from Arm River showing alternating quartzose layers with small scale kink folding.



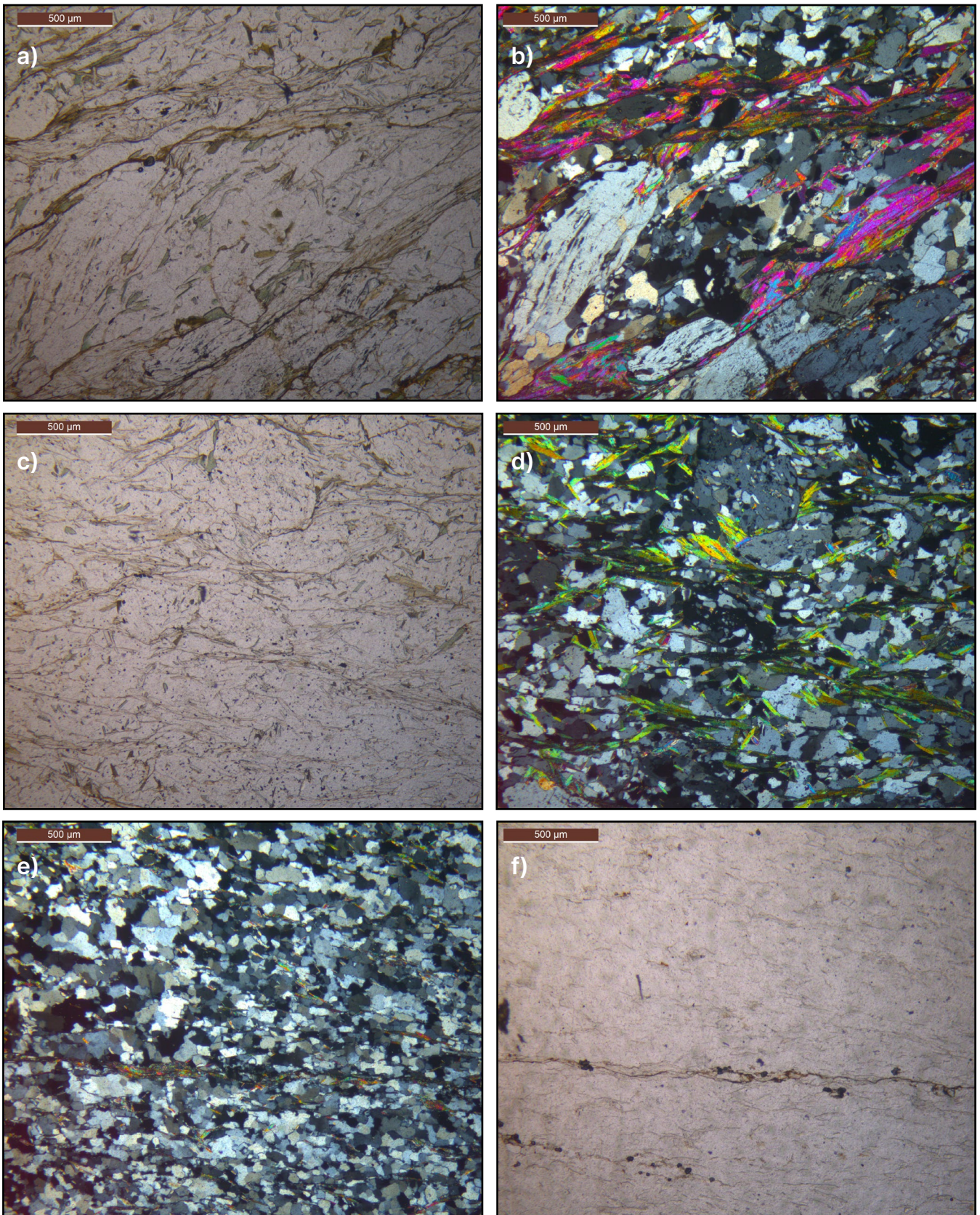


Figure 4. Photomicrographs of samples R030082 (a-d) and R030085 (e, f) showing quartz-mica schist and quartzite sampled for geochronology. a) Medium- to coarse-grained fabric comprising elongate, sutured quartz grains aligned parallel to foliation, with large muscovite laths and sparse chloritoid. Pressure solution seams and strain shadows reinforce the dominant foliation, photographed under normal light. b) The same image, under cross polarised light, showing albite porphyroblasts with curved inclusion trails, suggesting high-strain and possible shear band geometry. c) Fine-grained quartzite showing a mosaic of equant to slightly elongate quartz grains with undulose extinction and local poikilitic albite porphyroblasts under normal and (d) cross polarised light. e) Fine-grained quartzite exhibiting a granoblastic mosaic of equant quartz grains with undulose extinction. f) The same sample under normal light showing opaque phases aligned along the dominant foliation.

METHODS

Approximately 500 g of each sample were crushed using a hydraulic crusher and milled in a Cr-steel ring mill to a grain size $<400\ \mu\text{m}$. The samples were then individually panned for zircons using a gold pan under sterile conditions, with blank tests undertaken between each sample to ensure no cross-contamination of zircons between samples. Samples were dried and magnetic minerals were removed using a Fe-B-Nd hand magnet. The non-magnetic residue, containing the zircons, was poured onto an adhesive strip in a confined area of $\sim 3\text{--}5\ \text{mm}$ in diameter. 2.5 cm laser moulds were placed around the samples and epoxy resin was poured into the mould. The epoxy resin was left to cure at $60\ ^\circ\text{C}$ for 24 hours and then polished using a polishing lap.

Zircon grains were imaged in the Central Science Laboratory (CSL) at the University of Tasmania under cathodoluminescence (CL) using the FEI MLA650 environmental scanning electron microscope (E-SEM) (10.0 kV at a working distance of 14.5 mm). A grid reference system was designated for each sample, and 15–20 images were taken from each sample in sequential frames, with a horizontal field width (HFW) of $500\ \mu\text{m}$. These images were used to select zircons for laser ablation analysis.

The zircons were subsequently analysed for U-Pb data using laser ablation inductively coupled plasma mass spectrometry (LA-ICPMS). Zircons were ablated using a Coherent COM-Pex Pro ArF 193 nm wavelength Excimer laser operating with a 20 ns pulse width and $20\ \mu\text{m}$ spot size and analysed using an Argilent7900 mass spectrometer. Spot locations were pre-programmed using the stitched CL-SEM images to identify rims, cores and zoning with the zircon grains. 754 spots were programmed for ablation in the 2 samples, along with zircon standards (Temora: Black et al., 2003), Plesovice (Slama et al., 2008) and 91500 (Wiendenbeck et al., 1995).

Ninety to one hundred zircons were analysed for each sample producing 57 and 88 useful concordant analyses. All zircons lying on randomly orientated transects were programmed for ablation. None of the samples in this study yielded > 100 grains with robust U-Pb ages as recommended by Dodson (et al., 1988). This limitation must be considered in the interpretation of these results.

U-Pb data was reduced using LADR processing software, an in-house LA-ICPMS data set reduction programme (Norris and Danyushevsky, 2018). Results from LADR were sorted to remove and/or correct samples with unwanted transient spikes in isotopes caused by the ablation of inclusions within the zircon. Analyses were also corrected for data loss due to full penetration of the zircon by ablation. Reduced data was analysed and plotted using IsoplotR (Vermeesch, 2018) and DZstats v.2.2 (Saylor and Sundell, 2016). In zircon geochronology, $^{207}\text{Pb}/^{206}\text{Pb}$ ages are commonly used when ages exceed 1500 Ma, while the $^{206}\text{Pb}/^{238}\text{U}$ age is preferred for ages less than 1.5 Ga (Martin et al., 2011). However, where ages are clustered close to 1.5 Ga (as is the case here) mixing $^{207}\text{Pb}/^{206}\text{Pb}$ and $^{206}\text{Pb}/^{238}\text{U}$ ages may introduce artefacts in the zircon age distribution.

As the samples here are all Proterozoic ages less than 1 Ga are of little interest. For these reasons, all ages reported in this study are $^{207}\text{Pb}/^{206}\text{Pb}$ ages, unless specified otherwise. Histograms and KDEs of zircon ages were produced using the IsoplotR kernel density estimates (KDE) function (Vermeesch 2018b). The Wasserstein-2 test (Lipp and Vermeesch, 2023) was used to compare detrital zircon age distributions for the Multidimensional Scaling (MDS) map.

RESULTS

Numerical results for each sample are presented in [Table 2](#) and on Tera-Wasserbug concordia diagrams ([Figures 5](#) and [6](#)), and the original U/Pb ICPMS data is presented in [Appendix 1](#). For each individual zircon analysis, a “preferred age” was chosen based on the degree of discordance, the amount of common Pb and the age of the zircons. For most of the sample suite, $^{207}\text{Pb}/^{206}\text{Pb}$ ages are referred. For those analyses for which lead loss is identifiable, the preferred age has been taken as the $^{207}\text{Pb}/^{206}\text{Pb}$ age. The preferred zircon ages from each sample are also presented as probability density plots ([Figures 7](#) and [8](#)).

Dublin Road - Sample R030082

Of the 89 grains analysed from sample R030082, 32 analyses were excluded due to discordance. A single non-concordant Mesoproterozoic to Palaeoproterozoic zircon was identified at 1249.5 (Table 2). The next youngest zircons are 1311 and 1360 Ma, however these are off concordia (Figure 5) and were

Table 2. Summary of ages for the Northern Tyennan samples.

Analysis Number/ Sample Number	Lithology	Stratigraphic Unit	Youngest concordant ²⁰⁷ Pb/ ²⁰⁶ Pb zircon age (Ma) and uncertainty 2σ	Weighted mean age (Ma) with uncertainty (Ma) 2σ of youngest concordant zircons	Number of zircons used for age cal- culation/ total
2024-G-610/ R030082	Quartz muscovite schist	Mersey Metamorphic Complex	1431 ± 2.3	1435 ± 32 MSWD: 0.66	4/57
2024-G-611/ R030085	Quartzite	Mersey Metamorphic Complex	1419 ± 2.22	1449 ± 22 MSWD:2.37	4/88

omitted from the age calculation. There are a cluster of concordant zircons between 1440 and 1518 Ma. The remaining zircons span the largest population 1560 and 1822 Ma (n=51). The youngest group of concordant ages have a mean age of 1435 ± 32 Ma which is interpreted here as the maximum depositional age for this sample. There is a major age peak at ca. 1600 Ma (Figures 5 and 7) and minor age peaks at ca. 1500 Ma and 1700 Ma (with some 100 % concordant grains). There are five older grains with ²⁰⁷Pb/²⁰⁶Pb ages ranging from 2360 to 3120 Ma; but some of these are discordant and have higher levels of iron. The oldest concordant grain is 3210 ± 2 Ma (²⁰⁷Pb/²⁰⁶Pb).

Mersey Forest - Sample R030085

Of the 88 grains analysed from sample R030085, three analyses were excluded due to discordance. The two largest populations are a major Palaeoproterozoic population at 1589.9–1892 Ma (n=43) and a smaller Mesoproterozoic to Palaeoproterozoic population at 1520.1–1428.8 Ma (n=4). The youngest analysis yielded an age of 398.2 Ma, which is a far outlier from the next youngest analysis, and is interpreted to represent contamination (due to a Devonian age granite sample also occurring on the same mount), or may represent a grain reset during the Tabberaberan orogeny.

The ²⁰⁷Pb/²⁰⁶Pb ages are preferred for all the grains. The youngest concordant zircon is 1428.8 ± 1.8 Ma (Figure 6). There are four zircons with a median age of 1449 ± 22 Ma. The next youngest zircons (N=3) have a lower intercept age of 1558 ± 12 Ma. The lower intercept mean age of the most abundant zircons (N=43) in this sample is 1728 ± 4 Ma.

DISCUSSION

Dublin Road - Sample R030082

The detrital zircon age spectrum of sample R030082 from Dublin Plain is characterised by two principal components: a broad Palaeoproterozoic population (~1.55–1.80 Ga) and a

subordinate but well-defined Mesoproterozoic peak (~1.44–1.52 Ga). These features most closely resemble the zircon age signatures of the Pedder River Siltstone and Balfour Subgroup presented in Halpin et al. (2014). Both units exhibit abundant Palaeoproterozoic zircons, accompanied by a persistent ~1.45 Ga peak ages. However, R030082 lacks the slightly bimodal 1800 Ma component observed in the Pedder River Siltstone and Balfour Subgroup.

A small number of Archaean grains (>2.3 Ga) in R030082 indicate limited input from older basement sources. Similar low-frequency Archaean components are documented in western RCG units by Halpin et al. (2014), consistent with intermittent recycling of ancient crust rather than a major provenance contribution (Halpin et al., 2014). The youngest concordant population at ~1.45–1.50 Ga provides the most reliable constraint, placing deposition after ~1.46 Ga. KDE comparisons (Figure 9b and d and Figure 10) show that R030082 aligns most strongly with the Pedder River and Balfour Subgroup zircon populations, reflecting derivation from long-lived Palaeoproterozoic source terranes with a secondary Mesoproterozoic component.

A large peak at 1600 Ma, in the Laurentian Magmatic gap, was interpreted by Halpin et al. (2014) as typical of the oldest part of the Rocky Cape Group, below the Detention Subgroup. Tasmania was part of Nuna and close to Laurentian in the Mesoproterozoic (Mulder et al. 2019). In Laurentia, detrital zircons between 1610 and 1490 Ma are considered to come from a western source, probably the North Australian craton (Brennan et al., 2021). Zircons in the age range 1610 Ma to 1490 Ma are rare in the Belt Supergroup in rocks younger than 1430 Ma (Hirtz et al., 2024). The Detention Subgroup may be a chronostratigraphic correlate of the Missoula Group. On the other hand this provenance switch may occur at a different time in Tasmania. The palaeogeographic distance between Tasmania and the Belt–Purcell Basin at 1430 Ma remains uncertain.

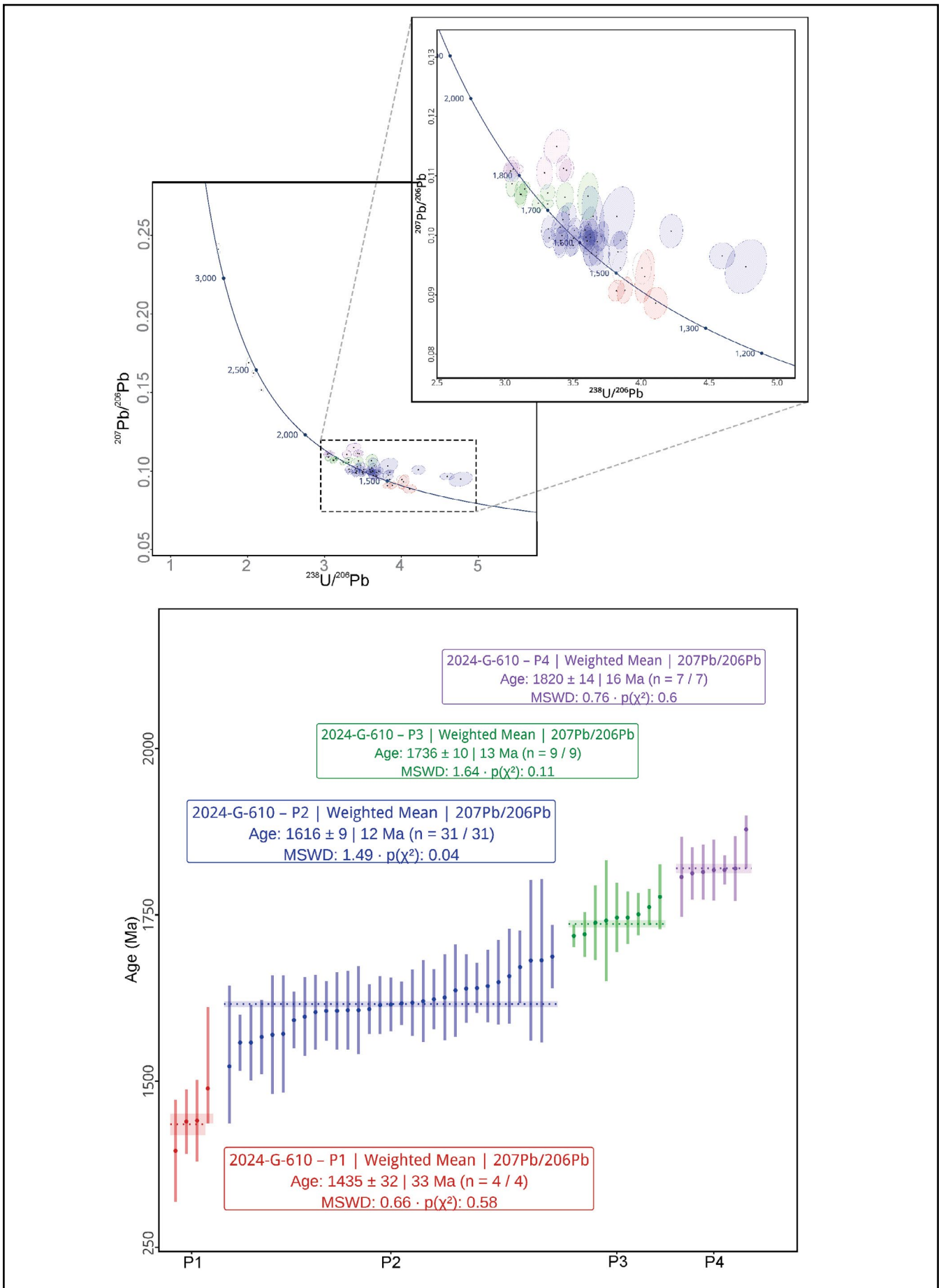


Figure 5. Tera-Wasserburg concordia diagram for detrital zircon U-Pb analyses from sample R030082 (Dublin Plain). The enlarged inset highlights the four youngest age populations identified in the dataset. Populations 1 to 4 (P1 to P4) are coloured and correspond with the weighted mean plot with each population, as shown below, with mean ages and MSWD values displayed for direct comparison. These age populations constrain the maximum depositional age and subsequent disturbance history for the quartz-mica schist facies near Dublin Plain.

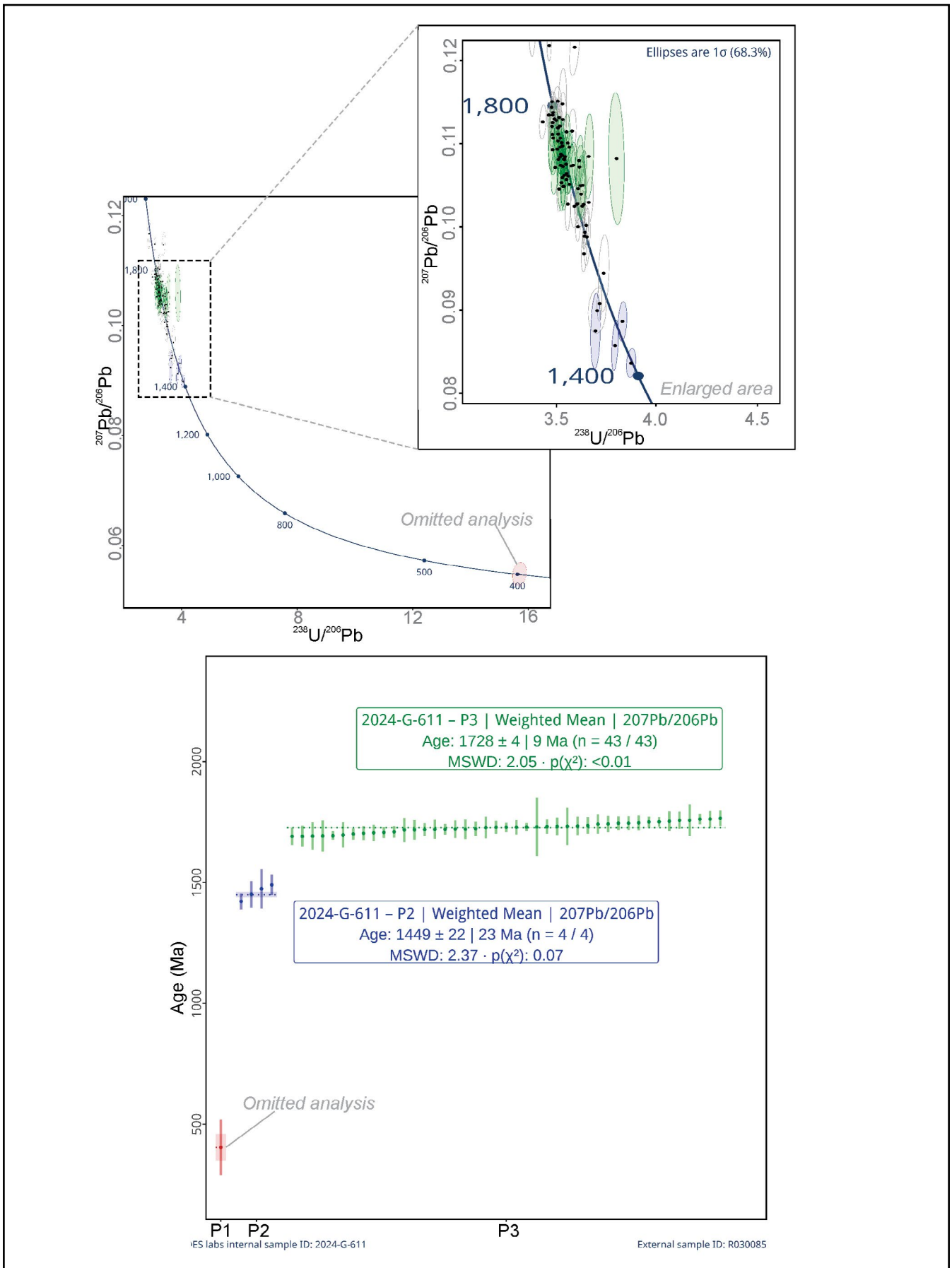


Figure 6. Tera-Wasserburg concordia diagram for detrital zircon U-Pb analyses from sample R030085 (Arm River). The inset highlights the youngest age populations distinguished in the dataset. Population 1 represents the youngest analyses and likely contamination (as a Devonian sample was included on the grain mount). Population 2 forms a concordant cluster, defining the most likely youngest concordant population in the sample. Population 3 comprises a moderately older group that shows greater dispersion away from concordia. Corresponding weighted mean plots for the three populations are shown below, with mean ages and MSWD values reported.

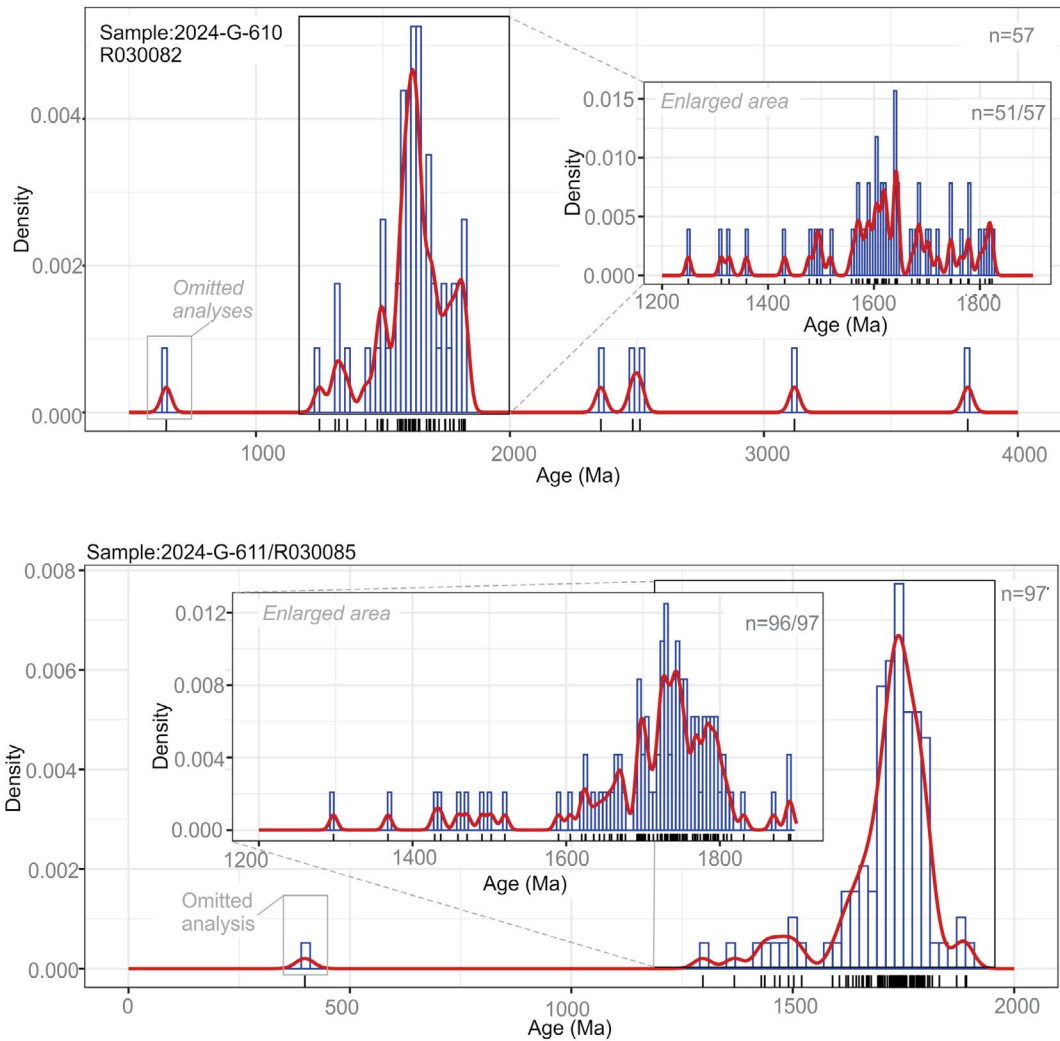


Figure 7. Probability density plots (histograms and KDE curves) of U–Pb LA ICP MS detrital zircon ages for samples R030082 (top) and R030085 (bottom) from the Northern Tyennan Region. For each sample, the main probability plot shows the full age range of analysed grains, with omitted or discordant analyses noted. Insets provide enlarged views of the principal Palaeoproterozoic and Mesoproterozoic age populations, illustrating the internal structure of the dominant age peaks. The KDE curves (red) and density histograms (blue) highlight the major zircon age modes characteristic of recycled Palaeoproterozoic–Mesoproterozoic sources. Sample R030082 displays major peaks between ca. 1.4–1.6 Ga and 1.6–1.8 Ga, with sparse older and younger grains. Sample R030085 shows tightly grouped Palaeoproterozoic populations between ca. 1.45–1.50 Ga and 1.6–1.8 Ga, with no significant Neoproterozoic component.

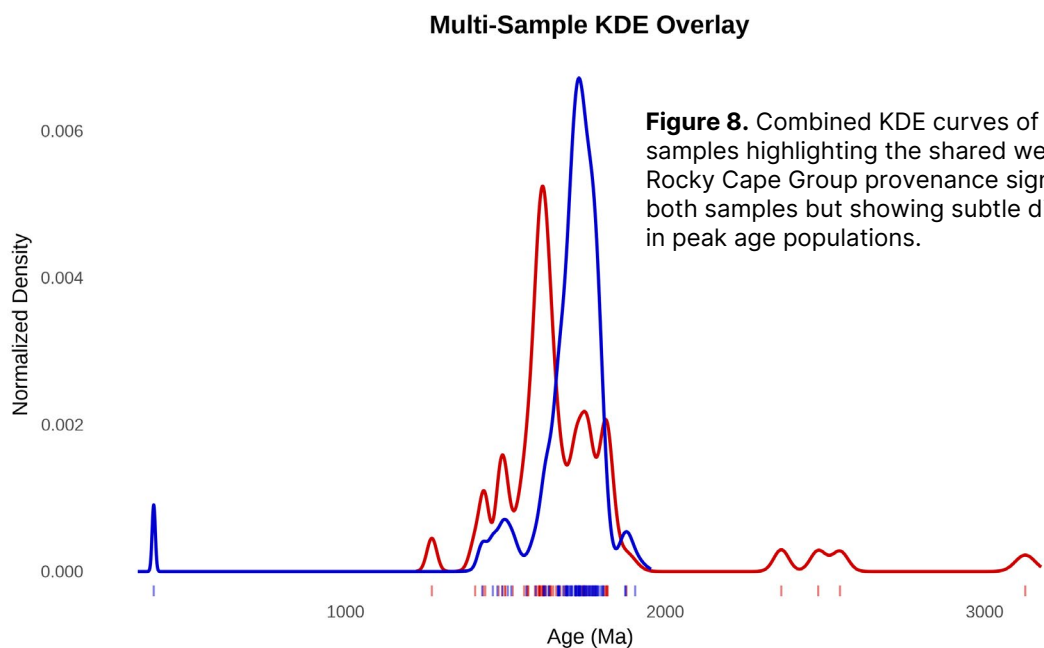


Figure 8. Combined KDE curves of both samples highlighting the shared western Rocky Cape Group provenance signature of both samples but showing subtle differences in peak age populations.

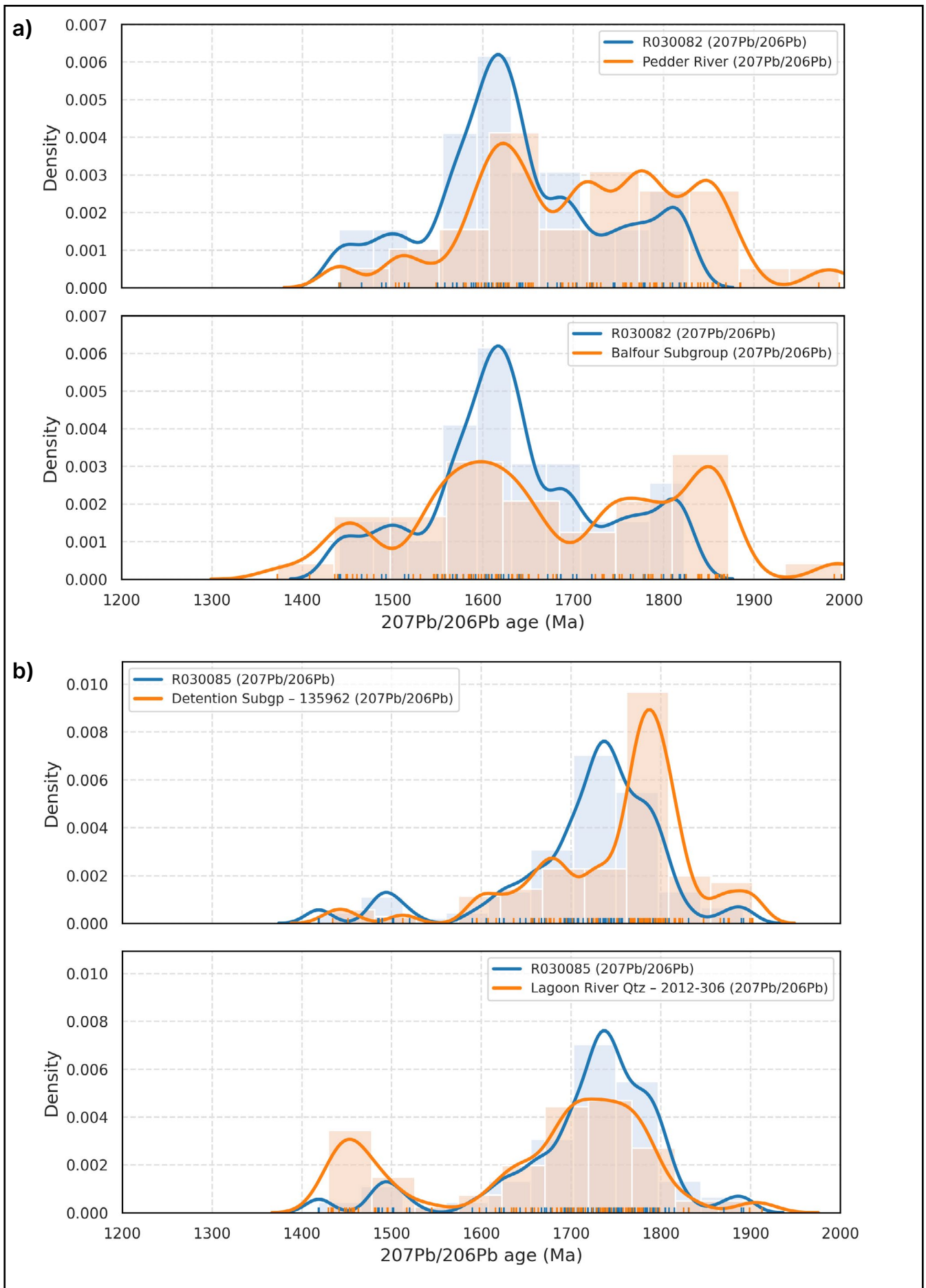


Figure 9. Comparative detrital zircon $^{207}\text{Pb}/^{206}\text{Pb}$ age distributions for samples R030082 (a), and R030085 (b) alongside representative units from Halpin et al. (2014). For R030085, comparisons are shown with the Detention Subgroup and Lagoon River Quartzite, b). For R030082, comparisons are shown with the Pedder River and Balfour Subgroup zircon suites (all sample data from Halpin et al., 2014).

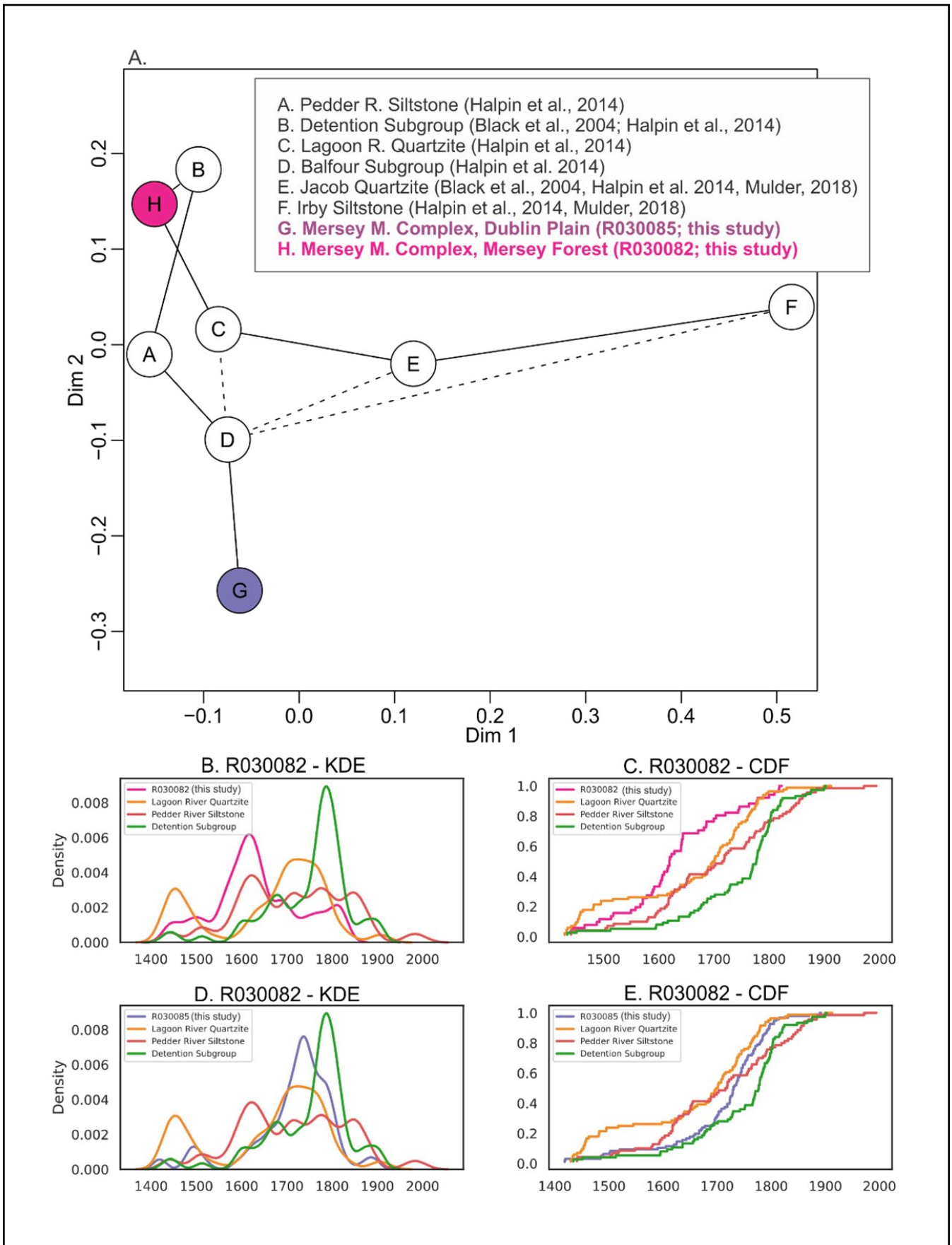


Figure 10. Provenance comparison of detrital zircon $^{207}\text{Pb}/^{206}\text{Pb}$ age spectra (1200–2000 Ma) for the Rocky Cape Group (RCG) and samples R030082 and R030085. (A) MDS plot of 90–110 % concordant analyses. Both samples plot nearest to Lagoon River Quartzite and Pedder River Siltstone fields, with Detention Subgroup slightly farther and upper RCG units (Irby Siltstone, Cowrie Siltstone, Jacob Quartzite) distinctly offset, indicating dissimilarity. (B–C) R030082 overlays: KDE and empirical CDF curves vs Lagoon, Pedder and Detention (KS values annotated). (D–E) R030085 overlays vs the same formations by KS and by a transparent mode-weighted score emphasizing the ~1.45 Ga and 1.55–1.80 Ga peaks. (F) Top-5 nearest formations by KS and by a transparent mode-weighted score emphasizing the ~1.45 Ga and 1.55–1.80 Ga peaks.

Mersey Forest- Sample R030085

The detrital zircon age distribution of sample R030085, with its dominant ~1.72 Ga peak and subordinate ~1.45–1.50 Ga population, closely match the broad 1.6–1.9 Ga and ~1460 Ma modes that characterise the Detention Subgroup (east and west), and also align well with the Lagoon River Quartzite, all of which display tightly clustered Palaeoproterozoic peaks accompanied by a consistent 1.45 Ga component (Figure 9b).

The KDE and MDS results (Figure 10) show that R030085 clusters strongly with samples characterised by major ~1.7 Ga peaks, including the Red Point Complex (Mulder, 2013), the Needles Quartzite and Tyennan Quartzite (Black et al., 2004), and the Strathgordon Metamorphic Complex (Black et al., 2004). These units all possess pronounced Palaeoproterozoic modes (between ~1.6 and 1.8 Ga; with peaks near ~1.7 Ga) which, in MDS space, plot adjacent to, and in some cases directly overlapping, the Mersey Forest sample (Figure 10B).

When compared with the Neoproterozoic successions discussed by Mulder et al. (2019), R030085 also shows similarities to allochthonous units of the Arthur Lineament, particularly the Keith Schist, which contains zircon spectra with a strong ~1.7 Ga and ~1.45 Ga age distribution, indicative of recycled Mesoproterozoic crust. R030085 shares this Mesoproterozoic provenance framework with the Oonah Formation sample, although this sample contains an additional Tonian (780–730 Ma) component related to syn-rift sedimentation. By contrast, R030085 lacks any Neoproterozoic detrital zircons, preserving a purely Mesoproterozoic–Palaeoproterozoic age distribution.

COMPARISON AND SUMMARY

Samples R030085 and R030082 both record a broad Palaeoproterozoic–Mesoproterozoic provenance characterised by abundant ~1.65–1.90 Ga zircons together with a consistent ~1.45 Ga population. This signature matches the dominant detrital components of the western lower–middle Rocky Cape Group (RCG) described by Halpin et al. (2014) and is consistent with sourcing from long-lived Palaeoproterozoic crustal provinces.

Within this framework, R030085 exhibits patterns that closely match the zircon populations of the Detention Subgroup and Lagoon River Quartzite (Figures 9 and 10) and also shows strong similarity to units with strong Palaeoproterozoic age signatures within the

Tyennan region (Figure 11A), including the Red Point Complex, Needles Quartzite, Tyennan Quartzite, and the Strathgordon Metamorphic Complex (Mulder, 2013 and Black et al., 2004). In contrast, KDE and MDS comparisons (Figures 9 and 10) show that R030082 aligns most strongly with the Lagoon River Quartzite and Pedder River Siltstone, whereas units such as the Irby Siltstone and Jacob Quartzite plot distinctly apart. These relationships reflect the close tracking of the Lagoon River Quartzite and Pedder River Siltstone age distributions between 1.2–2.0 Ga, consistent with the low K–S distances observed.

A notable distinction between the samples is the presence of a younger, non-concordant zircon cluster (~1.25–1.31 Ga) in R030082. The zircons show elevated U contents (248–291 ppm), and the filtered discordia array yields a lower intercept near ~540 Ma, indicating disturbance during Cambrian orogenesis (~500 Ma). This interpretation is supported by field relationships. Cambrian U–Pb disturbance is well documented elsewhere in western Tasmania, including in zircon in the Franklin Metamorphic Complex of the central Tyennan (Brown et al., 2024) and monazite in the Mersey Metamorphic Complex (Chmielowski, 2009). Thus, the youngest discordant ages in R030082 most likely reflect Cambrian Pb-loss rather than a shift in sediment provenance.

The prominent ~1.60 Ga mode in R030082 is typical of the oldest Rocky Cape Group (Halpin et al., 2014) and is consistent with paleogeographic models placing Tasmania near Laurentia within Nuna during the Mesoproterozoic (Mulder et al., 2019). The scarcity of 1610–1490 Ma zircons in Belt–Purcell Basin successions younger than ~1430 Ma (Hirtz et al., 2024) suggests that regional provenance transitions did not occur uniformly throughout Nuna and the exact position of Tasmania in relation to protoliths of the Belt–Purcell Supergroup remain unclear.

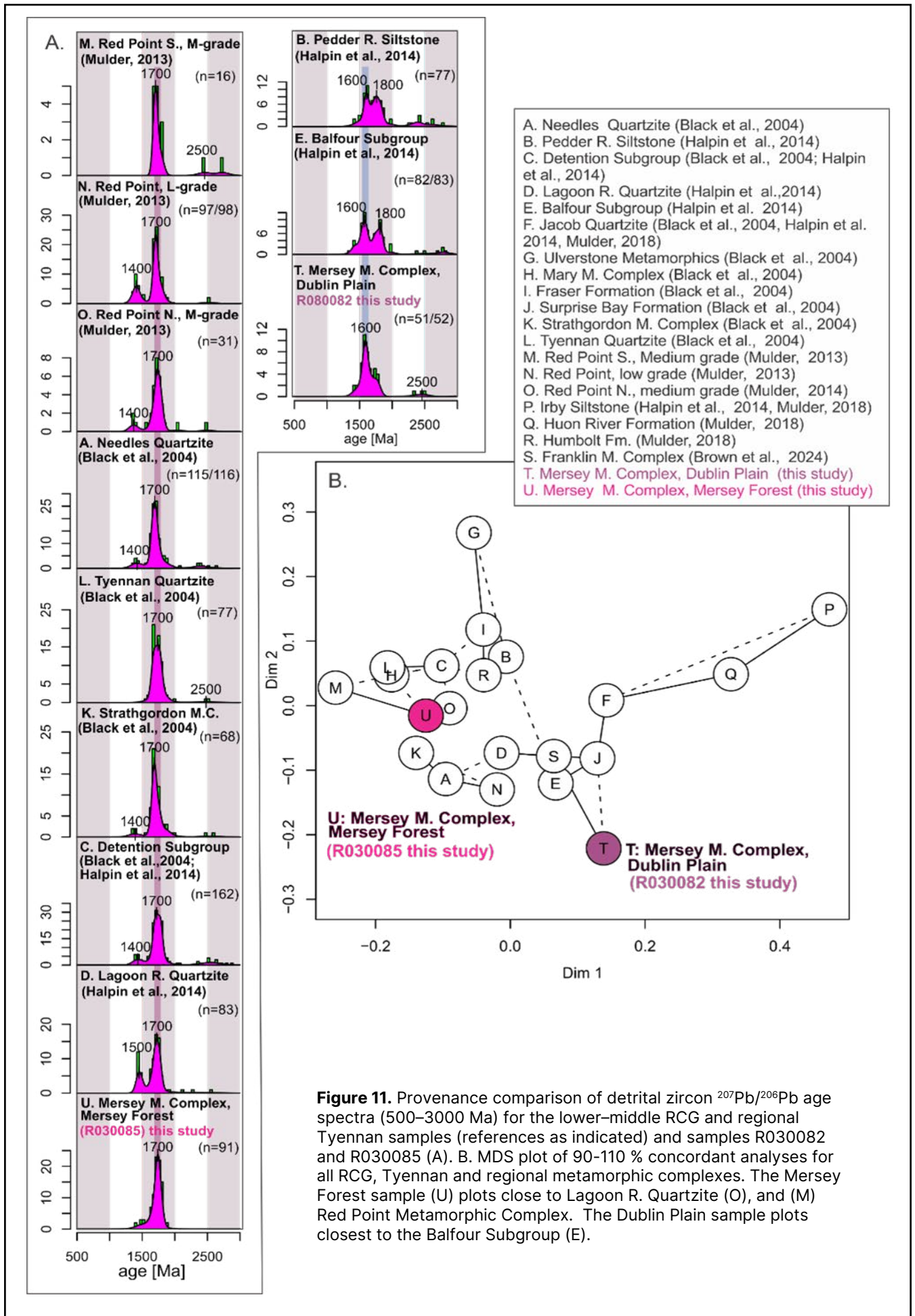


Figure 11. Provenance comparison of detrital zircon $^{207}\text{Pb}/^{206}\text{Pb}$ age spectra (500–3000 Ma) for the lower–middle RCG and regional Tyennan samples (references as indicated) and samples R030082 and R030085 (A). B. MDS plot of 90–110 % concordant analyses for all RCG, Tyennan and regional metamorphic complexes. The Mersey Forest sample (U) plots close to Lagoon R. Quartzite (O), and (M) Red Point Metamorphic Complex. The Dublin Plain sample plots closest to the Balfour Subgroup (E).

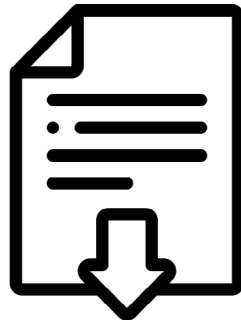
REFERENCES

- Black, L. P.**, Calver, C. R., Seymour, D. B., and Reed, A. 2004. SHRIMP U–Pb detrital zircon ages from Proterozoic and Early Palaeozoic sandstones and their bearing on the early geological evolution of Tasmania. *Australian Journal of Earth Sciences*, 51, 885–900.
- Black, L. P.**, Kamo, S. L., Allen, C. M., Aleinikoff, J. N., Davis, D. W., Korsch, R. J., and Foudoulis, C. 2003. TEMORA 1: a new zircon standard for Phanerozoic U–Pb geochronology. *Chemical Geology*, 200, 155–170.
- Brennan, D. T.**, Mahoney, J. B., Li, Z.-X., Link, P. K., Evans, N. J., and Johnson, T. E. 2021. Detrital zircon U–Pb and Hf signatures of Paleo-Mesoproterozoic strata in the Priest River region, northwestern USA: A record of Laurentia assembly and Nuna tenure. *Precambrian Research*, 367, <https://doi.org/10.1016/j.precamres.2021.106445>
- Brown, D. A.**, Hand, M., and Morrissey, L. J. 2021. Zircon petrochronology and mineral equilibria of the eclogites from western Tasmania: Interrogating the early Palaeozoic East Gondwana subduction record, *Gondwana Research*, 93, 252–274, <https://doi.org/10.1016/j.gr.2021.02.015>
- Chmielowski, R.** 2009. *The Cambrian Metamorphic History of Tasmania*. PhD thesis. University of Tasmania.
- Cumming, G. V.** in prep. 2026. *Borradaile 1:25,000 geological map sheet*. Mineral Resources Tasmania.
- Dodson, M. H.**, Compston, W., Williams, I. S., and Wilson, J. F. 1988. A search for ancient detrital zircons in Zimbabwean sediments. *Journal of the Geological Society*, 145(6), 977–983. <https://doi.org/10.1144/gsjgs.145.6.0977>
- Halpin, J. A.**, Jensen, T., McGoldrick, P., Meffre, S., Berry, R. F., Everard, J. L., Calver, C. R., Thompson, J., Goemann, K., and Whittaker, J. M. 2014. Authigenic monazite and detrital zircon dating from the Proterozoic Rocky Cape Group, Tasmania: links to the Belt–Purcell Supergroup, North America. *Precambrian Research*, 250, 50–67.
- Hirtz, J. A. M.**, Constenius, K. N., Horton, B. K., Valencia, V. A., and Pratt, B. R. 2024. Continental scale drainage reorganization during Mesoproterozoic orogenesis: Evidence from the Belt Basin of western North America: *Geosphere*, 20, 4, p. 1133–1161, <https://doi.org/10.1130/GES02732.1>
- Jennings, I. B.** 1963. Explanatory Report: Middlesex: One Mile *Geological Map Series* (Sheet K55-6-45). Tasmania Department of Mines, Geological Survey.
- Lipp, A.**, and Vermeesch, P. 2023. Short communication: The Wasserstein distance as a dissimilarity metric for comparing detrital age spectra and other geological distributions. *Geochronology*, 5(1), 263–270. <https://doi.org/10.5194/gchron-5-263-2023>
- Martin, A. J.**, Gehrels, G. E., and DeCelles, P. G. 2011. Detrital zircon geochronology of pre-Tertiary strata in the Tibetan-Himalayan orogen. *Tectonics*, 30(5). <https://doi.org/10.1029/2011TC002868>
- Mattner, S.** 2015. *Geological and geochronological constraints on the Precambrian basement and island arc collision at Lake Rowallan, Tasmania*. Honours Thesis, University of Tasmania.
- Meffre, S.**, Berry, R. F., and Hall, M. 2000. Cambrian metamorphic complexes in Tasmania: tectonic implications. *Australian Journal of Earth Sciences*, 47, 971–985.
- Mulder, J. A.** 2013. *The structure, metamorphism and geochronology of the metamorphic rocks of the Port Davey–South Coast region, SW Tasmania*. Honours Thesis, University of Tasmania.
- Mulder, J. A.**, Halpin, J. A., and Daczko, N. R. 2015. Mesoproterozoic Tasmania: Witness to the East Antarctica–Laurentia connection within Nuna. *Geology*. <https://doi.org/10.1130/G36850.1>
- Mulder, J. A.**, Karlstrom, K. E., Fletcher, I. R., Meffre, S., Halpin, J. A., Tsansis, B. and Berry, R. F. 2018. The Rocky Cape Group, Tasmania: A link between the sedimentary successions of western Laurentia and East Antarctica in the Mesoproterozoic. *Precambrian Research*, 308, 18–33.

- Mulder, J. A.**, Everard, J. L., Cumming, G. V., Meffre, S., Bottrill, R., Meredith, A. S., Halpin, J. A., McNeill, A. W., and Cawood, P. A. 2019. Neoproterozoic opening of the Pacific Ocean recorded by multi-stage rifting in Tasmania, Australia. *Earth Science Reviews*, 201. <https://doi.org/10.1016/j.earscirev.2019.103041>
- Norris, A.**, and Danyushevsky, L. 2018. *LADR: LA-ICP-MS Data Reduction Software*. Norris Scientific.
- Saylor, J. E.**, and Sundell, K. E. 2016. Quantifying comparison of detrital zircon age distributions. *Geosphere*, 12(2), 587–620.
- Sláma, J.**, Košler, J., Condon, D. J., Crowley, J. L., Gerdes, A., Hanchar, J. M., and Whitehouse, M. J. 2008. Plešovice zircon — A new natural reference material for U–Pb and Hf isotopic microanalysis. *Chemical Geology*, 249(1–2), 1–35.
- Spry, A. H.** 1958. The geology of the Mersey-Forth area. Hydro-Electric Commission Report (unpublished), Hobart, Tasmania.
- Turner, N. J.** 1989. Precambrian Rocks. In Burrett, C. F., & Martin, E. L. (Eds.), *The Geology and Mineral Resources of Tasmania. Geological Society of Australia Special Publication*, 15, 5–46.
- Vermeesch, P.** 2018. IsoplotR: A free and open toolbox for geochronology. *Geoscience Frontiers*, 9(5), 1479–1493.
- Wiedenbeck, M.**, Hanchar, J., Peck, W. H., Sylvester, P., Valley, J., Whitehouse, M., Kronz, A., Morishita, Y. and Nasdala, L. 2005. Further characterization of the 91500 zircon crystal. *Geostandards and Geoanalytical Research*, 28, 8–39.

APPENDIX 1

U/Pb ICPMS data



Download .xlsx data file



Tasmanian
Government

Mineral Resources Tasmania

PO Box 56 Rosny Park
Tasmania Australia 7018
Ph: +61 3 6165 4800
info@mrt.tas.gov.au